Bioorganic & Medicinal Chemistry Letters 21 (2011) 2785–2805

Contents lists available at ScienceDirect

Bioorganic & Medicinal Chemistry Letters

journal homepage: www.elsevier.com/locate/bmcl

Bioorganic & Medicinal Chemistry Letters Volume 21, Issue 10, 2011

Contents

ARTICLES

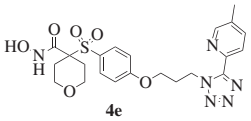

4e

MMP-13 = 0.60 nM
MMP-2 = 400 nM
MMP-8 = 250 nM

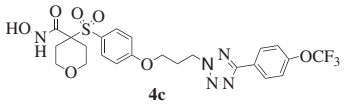

4c

MMP-13 = 0.13 nM
MMP-2 = 230 nM
MMP-8 = 80 nM

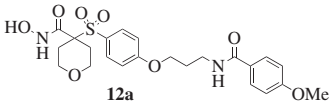

12a

MMP-13 = 1.6 nM
MMP-2 = 550 nM
MMP-8 = 900 nM
MMP-1 > 5000 nM
MMP-14 >5000 nM

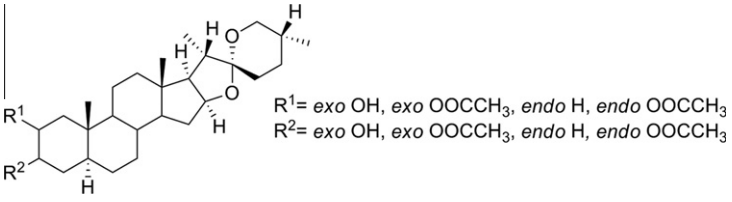

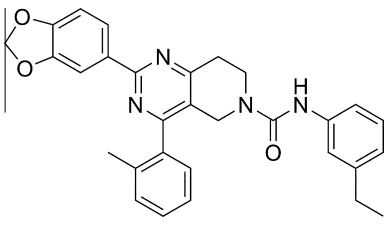

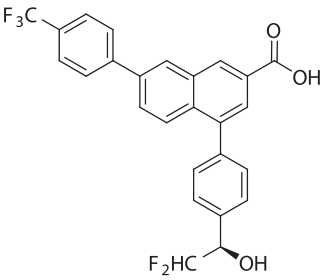

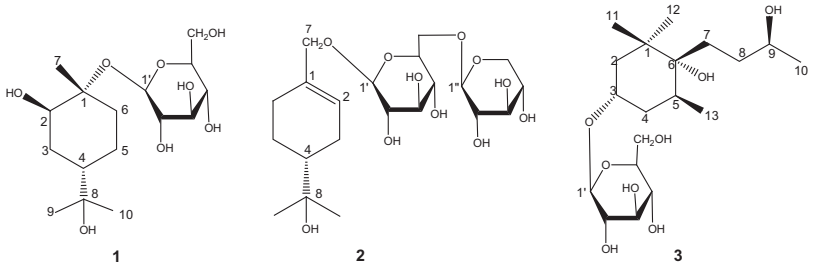

1 2 3

Two new monoterpene glycosides, distyloside A–B (**1**–**2**), and a new megastigmane glucoside, *iso*-dihydrodendranthemoside A (**3**) were isolated from twigs and leaves of *Distylium racemosum* Siebold & Zucc. (Hamamelidaceae).

A new unusual sterol, named lobophytosterol (**1**), and five known metabolites (**2**–**6**) were isolated from the methanol extract of the soft coral *Lobophytum laevigatum*. Compounds **1**–**3** showed cytotoxic activity against selected human cancer cell lines. Treatment of these cells with compound **1** resulted in an induction of apoptosis evident by chromatin condensation in treated cells. Besides, compounds **2**, **4**, and **6** significantly upregulated PPARs transcriptional activity dose-dependently in Hep-G2 cells.

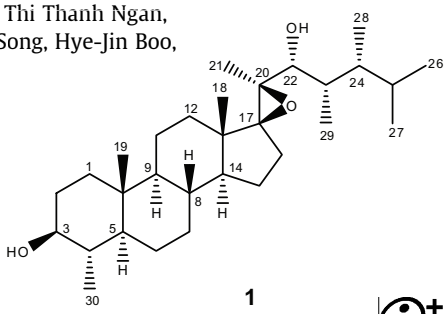

1

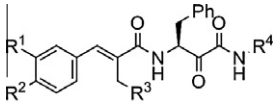

4

The excessive calpain activation causes serious cellular damage or even cell death in neurological disorders. Oxidative stress has also been implicated in the initiation or progression of neurodegenerative diseases. In the present study, a series of cinnamoyl ketoamides **4a**–**4j** were synthesized as hybrid structures of antioxidants and calpain inhibitors. Among synthesized, compound **4e** was the most potent inhibitor of μ-calpain (IC_{50} = 0.13 μM) and also exhibited strong antioxidant activities in three assay systems.

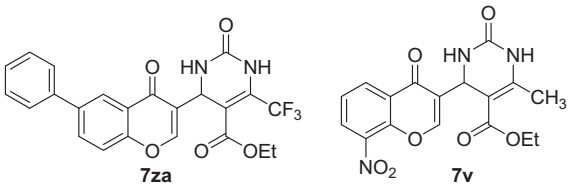

7za **7v**

Series of 4*H*-chromen-1,2,3,4-tetrahydropyrimidine-5-carboxylate derivatives were synthesized, screened for their anti-mycobacterial and anticancer activities, among them compound **7za** is more potent anti-mycobacterial, **7v** more potent anticancer agents compared to standard drugs and are being reported in this study for the first time to serve as a model compounds for design and development of therapeutic based anti-mycobacterial and anticancer activity.

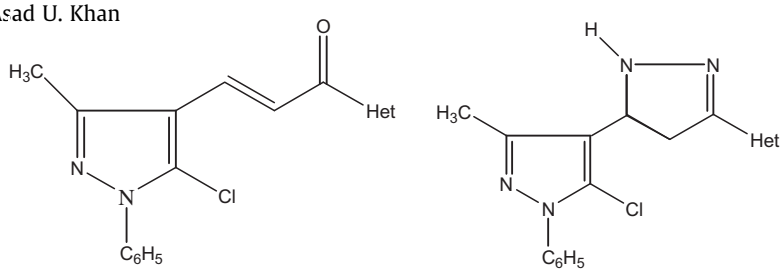

3a-c **4a-c**

A novel series of pyrazolyl chalcones (**3a–c**) and pyrazolines (**4a–c**) were synthesized under thermal solvent-free condition and were screened for their in vitro antibacterial and antifungal activities.

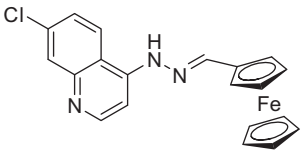

CMI = 2.5 - 5 μg/mL
Mycobacterium tuberculosis

Presented is the identification and evaluation of a novel series of (*E*)-3-(1-cyclohexyl-1*H*-pyrazol-3-yl)-2-methylacrylic acid derivatives identified from a deannulation study performed on the reported benzimidazole NS5B inhibitor, **1**. This resulted in the identification of (*E*)-3-(2-(4-((4′-cyano-4-(4-hydroxypiperidine-1-carbonyl)biphenyl-2-yl)-methoxy)phenyl)-1-cyclohexyl-1*H*-imidazol-4-yl)-2-methylacrylic acid (**11**) as a potent inhibitor of NS5B. Potential pathways for the further optimization of this series are suggested.

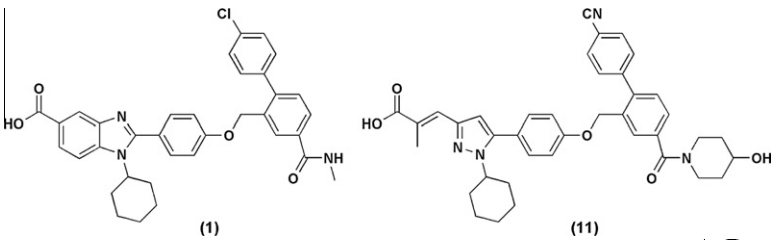

(1) **(11)**

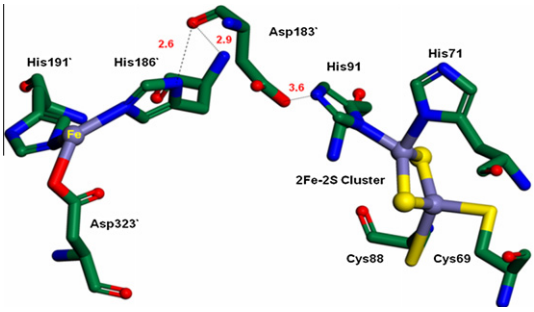

The electron in the PrnD Rieske oxygenase can be transferred by either of two pathways, one involving Asp183′ and the other involving Asn180′.

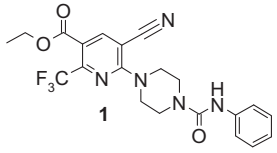

A novel series of piperazinyl-pyridine ureas, exemplified by **1**, was discovered to be $P2Y_{12}$ antagonists. SAR investigations presented several compounds with potencies in the sub-micromolar range. The pyridine 3-ethoxycarbonyl substituent, the urea *N–H* of the linker, and the right-hand aromatic ring all contributed significantly to potency. Solubility could be increased by shifting from 2-CF_3/5-CN to 2-H/5-Cl pyridines.

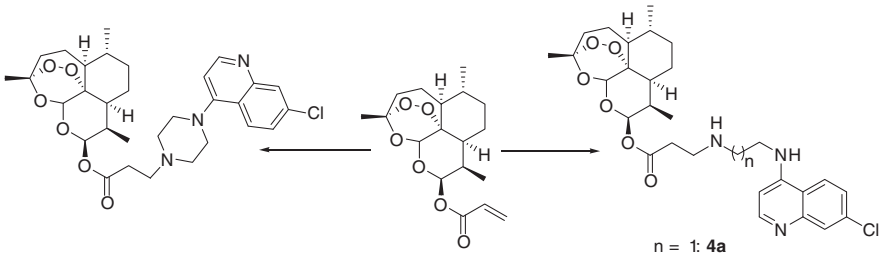

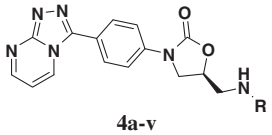

The synthesis and antibacterial activity of 3-(4-([1,2,4]triazolo[4,3,*a*]pyrimidin-3-yl)-phenyl)oxazolidin-2-ones is reported.

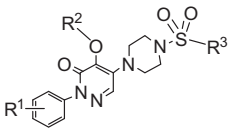

A series of small molecular pyridazinone analogs has been studied as potent β-1,3-glucan synthase inhibitors.

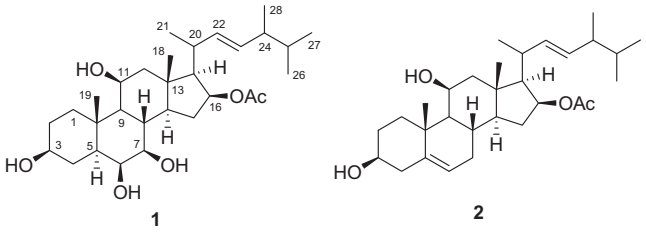

1 **2**

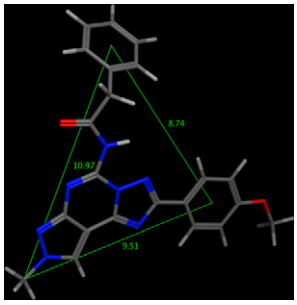

The ligand-based pharmacophore elucidation performed on 2-aryl-pyrazolo-triazolo-pyrimidines as potent hA_3 adenosine receptor antagonists has provided new insights on the structural characteristics deemed critical for the affinity at the hA_3 adenosine receptor.

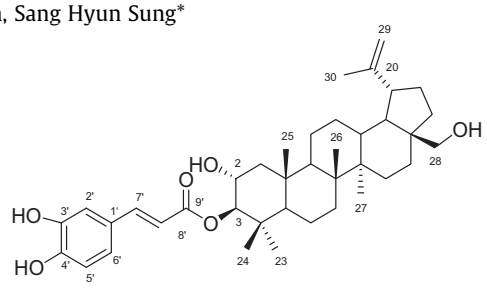

13

A new triterpenoid characterized as lup-20(29) en-2,28-diol-3-yl caffeate was isolated with 12 known diarylheptanoids from the barks of *Alnus firma*. Antifibrotic constituents of *A. firma* on HSCs might suggest the therapeutic potentials against liver fibrosis.

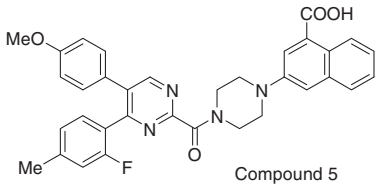

Compound 5

A series of six-membered heterocycle carboxamides were synthesized and evaluated as cholecystokinin 1 receptor (CCK1R) agonists. A pyrimidine core proved to be the best heterocycle, and SAR studies resulted in the discovery of analog **5**, a potent and structurally diverse CCK1R agonist.

Novel 5-(2-hydroxyphenyl)-3-methyl-4,5-dihydropyrazol-1-yl-anone as potential telomerase inhibitors were synthesized. The bioassay tests show that compound **4a** exhibited high activity against human gastric cancer cell SGC-7901, Hep-G2 and PC-3 cell lines. All title compounds were assayed for telomerase inhibition, the results show that compound **4a** can inhibit telomerase. Docking simulation was performed to position compound **4a** into the telomerase (3DU6) active site to determine the probable binding model.

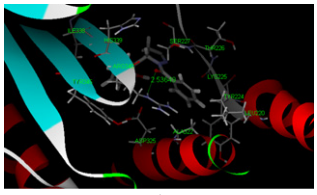


4a

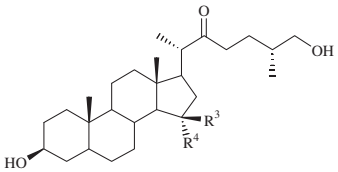

28: R^3=H,R^4=S3'; **29:** R^3=H,R^4=S4';
32: R^3=S3',R^4=H; **33:** R^3=S4',R^4=H;

S3'= 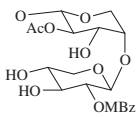

S4'= 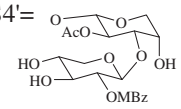

Eight 15(α)β-*O*-glycosyl 5(6)-dihydro-OSW-1 analogs bearing three kinds of disaccharide side chains were synthesized and evaluated for their antitumor activities.

Presented are initial SAR studies on a series of bridged 2-arylindole-based NS5B inhibitors. The introduction of bridging elements between the indole N1 and the *ortho*-position of the 2-aryl moiety results in conformationally constrained heterocycles that possess multiple additional vectors for further exploration. The binding mode and pharmacokinetic (PK) properties of select examples are reported.

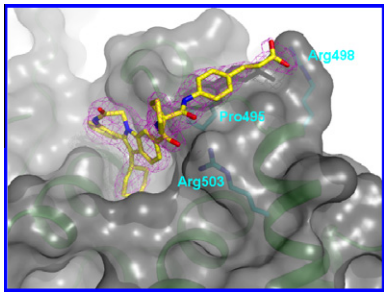

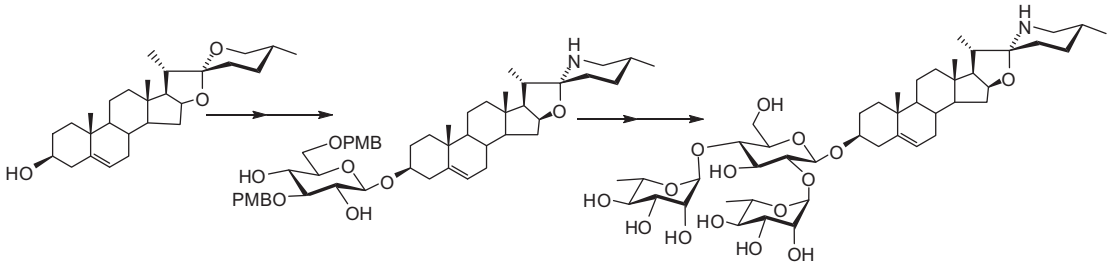

Solamargine has been synthesized in 13 steps and 10.5% overall yield from the natural abundant diosgenin.

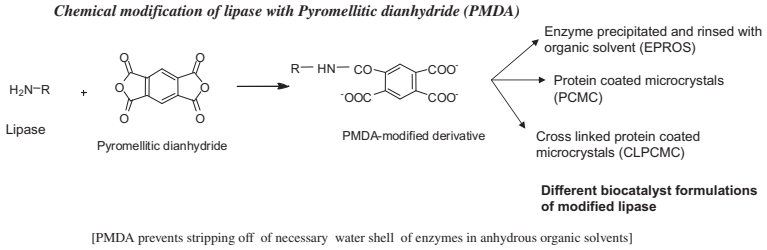

[PMDA prevents stripping off of necessary water shell of enzymes in anhydrous organic solvents]

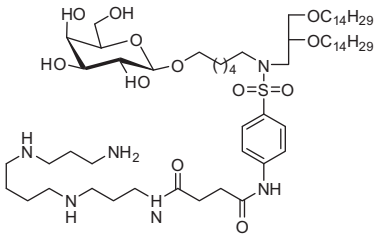

1

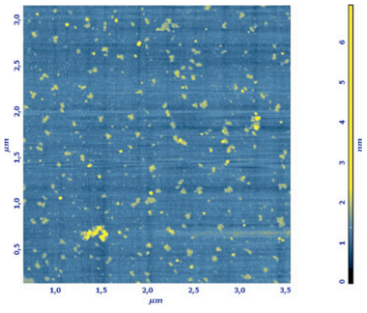

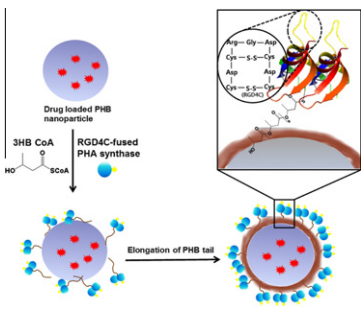

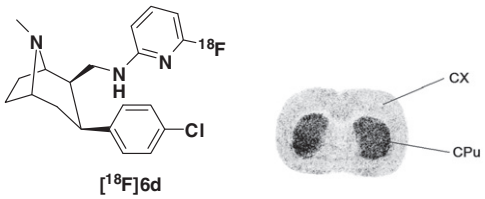

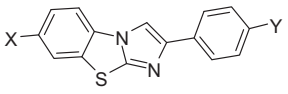

2-aryl-imidazo[2,1-*b*]benzothiazole

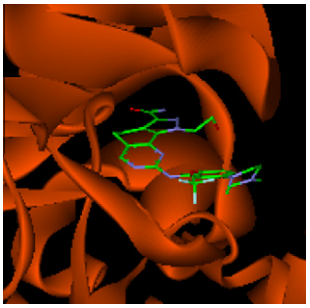

Lead optimization work on the 4,5-dihydro-1*H*-pyrazolo[4,3-*h*]quinazoline series led to identification of NMS-P937. Crystal structure of NMS-P937 with PLK1 was obtained and discussed. NMS-P937 is a potent, selective and orally available PLK1 inhibitor that is presently in Phase I clinical trials.

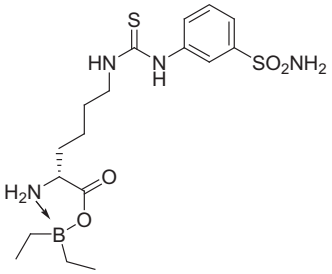

K_I (hCA I) = 3870 nM; K_I (hCA II) = 88 nM; K_I (hCA IX) = 9.5 nM; K_I (hCA XII) = 7.1 nM.

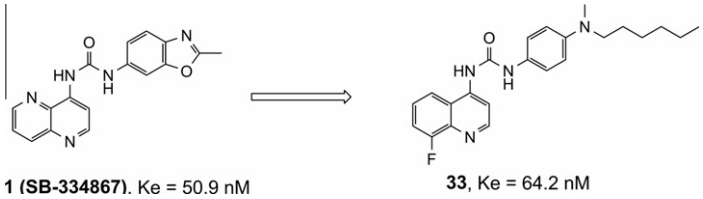

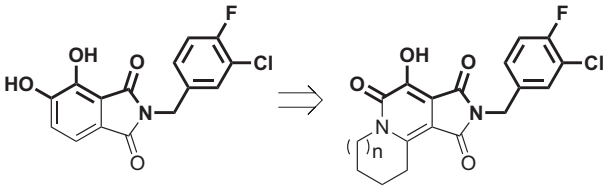

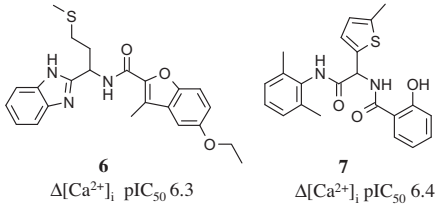

The identification of two novel series of formyl peptide receptor 1 (FPR1) antagonists are reported, represented by methionine benzimidazole **6** and diamide **7**. Both series specifically inhibited the binding of labelled fMLF to hrFPR1 and selectively antagonized FPR1 function in human neutrophils, making them useful in vitro validation tools for the target.

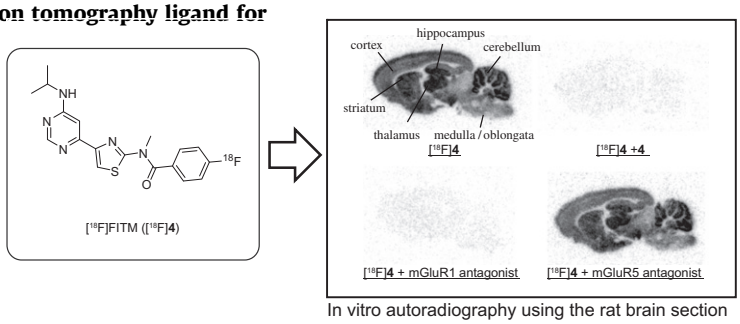

In vitro autoradiography using the rat brain section

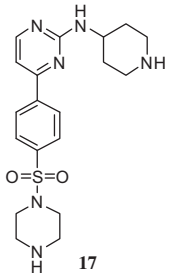

17

Piperidinyl aminopyrimidine derivatives as IKK-2 inhibitors were synthesized and their biological results were reported.

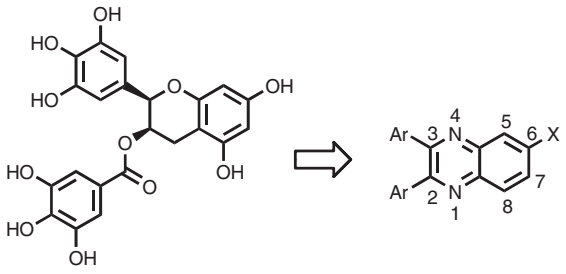

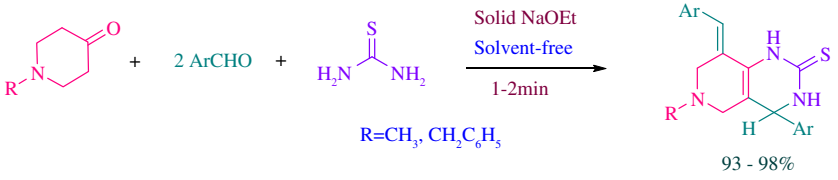

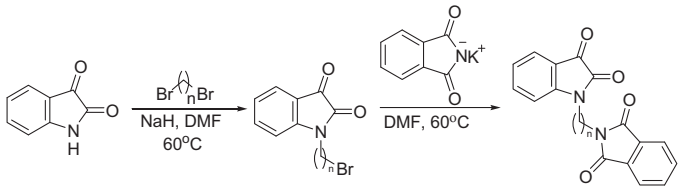

The manuscript pertains to the synthesis and in vitro cytotoxic evaluation of a series of *N*-alkylbromo and *N*-alkylphthalimido-isatins against four different human cancer cell lines. The active analogue **IS-4** exhibited IC_{50} values of 4.57, 10.90, 11.75, 12.40 and 54.20 μM against HeLa, PC-3, HCT-15, THP-1 and Colo-205, respectively.

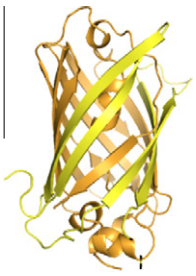

The crystal structure of reassembled fluorescent protein, Venus.

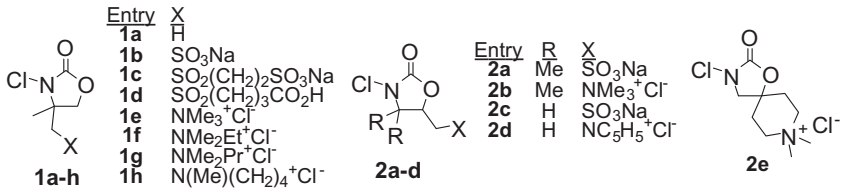

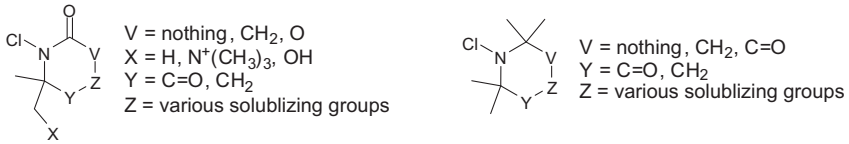

A novel series of *N*-chloroheterocycles has been prepared and the biological properties are reported.

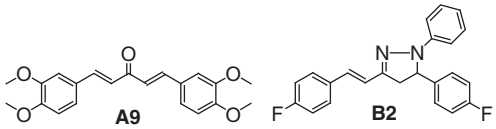

A9: IC_{50}^{3D7} = 1.97 μM, IC_{50}^{RKL9} = 1.69 μM; **B2**: IC_{50}^{3D7} = 9.10 μM, IC_{50}^{RKL9} = 11.09 μM. The synthesis and antimalarial activity of a series of dibenzylideneacetones and their pyrazolines are discussed.

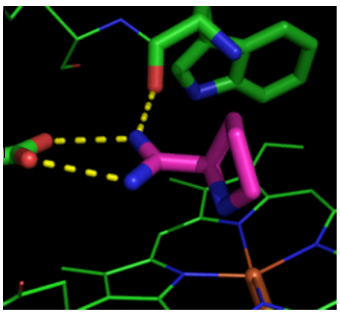

The exploration of heterocyclic carboxamidines as iNOS inhibitors led to the identification of (2*R*)-2-pyrrolidinecarboxamidine as a potent and selective haem-co-ordinating inhibitor.

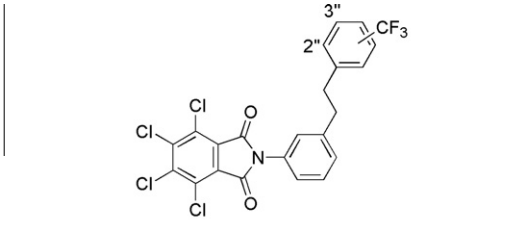

non-competitive and selective DPP-IV inhibitors

28a (3"-substituted) : DPP-IV IC_{50} = 3.1 μM, DPP-8 IC_{50} >30 μM
28b (2"-substituted) : DPP-IV IC_{50} = 4.0 μM, DPP-8 IC_{50} = 11 μM

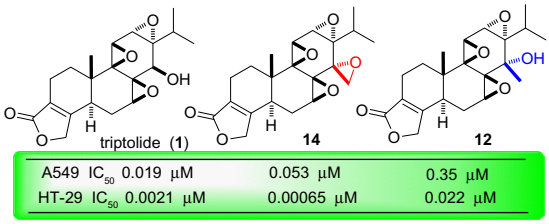

Triptolide γ-lactone and C-14 analogues were prepared and evaluated cytotoxity against A549 and HT-29 cells.

Fragment based screening using Surface Plasmon Resonance (SPR) followed by Pim-1 biochemical assay identified hit **10**. A X-ray structure of the bound complex of **10** to the Pim-1 protein revealed that **10** binds in the ATP binding site with the 5-bromo group sitting in the hydrophobic pocket near the hinge region. Guided by the X-ray structures, a potent Pim-1 inhibitor **38** was identified by adding an aminocyclohexylamino group at the 7-position of the benzofuran core. X-ray structure of the bound complex of **38** indicated that the terminal amino group forms salt-bridge interacts with *D128* and *E171* of the ribose binding site.

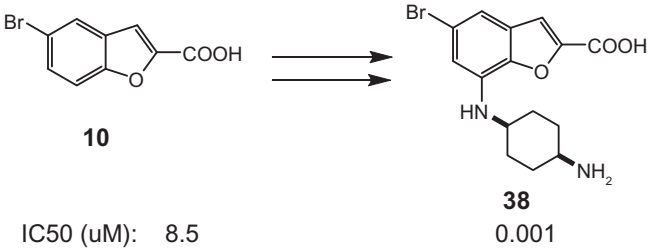

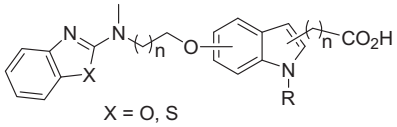

Synthesis of series of benzoxazole or benzothiazole containing indole-based analogs, 6-alkoxyindole-2-carboxylic acids and 5-alkoxy-3-indolylacetic acids, and their PPARγ/δ transactivation activities are reported.

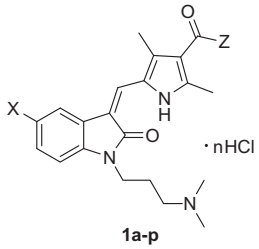

We report herein a series of novel 1-[3-(dimethylamino)propyl]indolin-2-one derivatives. Results revealed that all compounds show potent antitumor activity, compounds **1e**–**h** (IC_{50}'s: 0.45–5.08 μM) are more active than Sunitinib (IC_{50}'s: 1.35–6.61 μM), and the most active compound **1h** (IC_{50}: 0.47–3.11 μM) is 2.1–4.6-fold more potent than Sunitinib against all five cancer cell lines. In addition, **1a**–**p** have higher selectivity on VEGF-stimulated HUVEC other than bFGF-stimulated HUVEC.

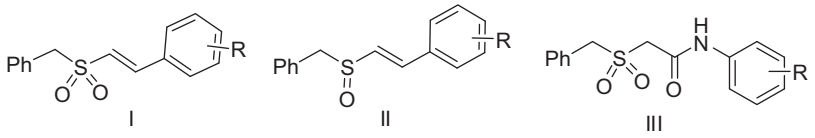

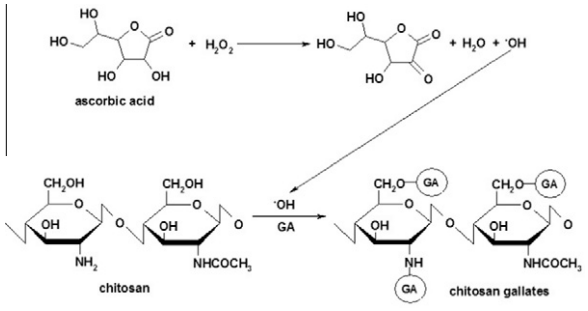

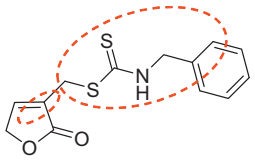

I-14

Broad spectrum anti-cancer activity IC_{50}<10μg/mL.

Three series of butenolide-containing dithiocarbamates were designed and synthesized. Their anti-tumor activity in vitro was evaluated. Among them compound **I-14** exhibited excellent anti-cancer activity against five human cancer cell lines with IC_{50} <10 μg/mL. Structure–activity relationship analysis showed that the introduction of dithiocarbamate side chains on the C-3 position of butenolide was crucial for anti-tumor activity.

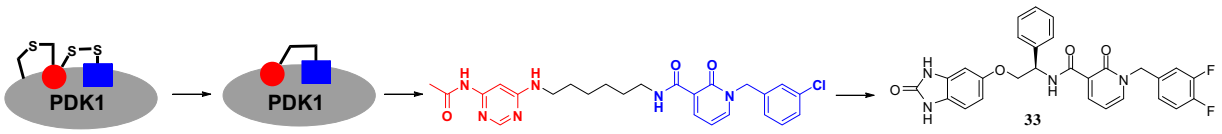

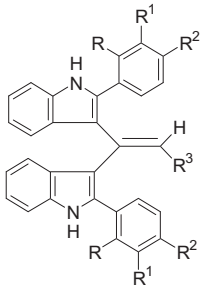

Synthesis and study of cytotoxic activity of 2,2′-diphenyl-3,3′-diindolylethylene derivatives are reported.

Novel potent inhibitors of 3C-like protease ($3CL_{pro}$) of severe acute respiratory syndrome associated coronavirus (SARS-CoV) were identified through structure-based virtual screening and validated the inhibitory activity in vitro.

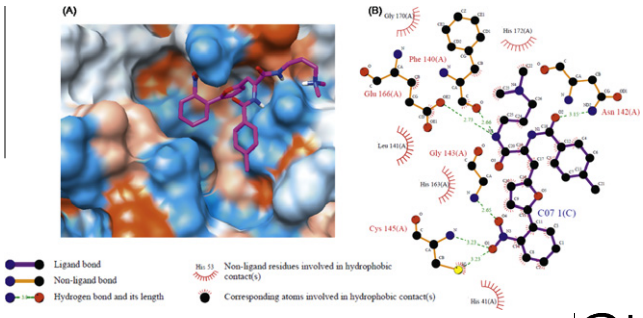

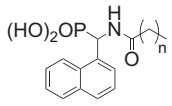

n = 10: K_i (red kidney bean PAP) = **5 μM**
n = 12: K_i (pig PAP) = **8 μM**

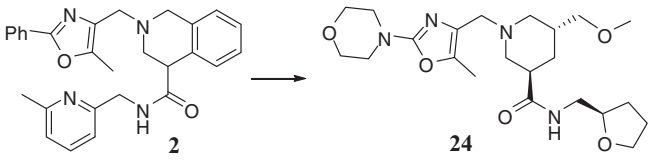

2 **24**

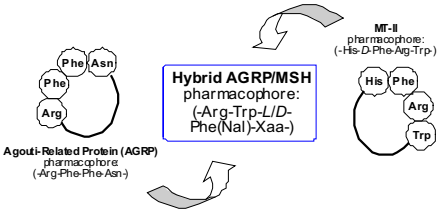

Design and synthesis of cyclic lactam hybrid α-MSH/Agouti-related protein (AGRP) analogues with high nanomolar range binding affinities at the hMC3–5R and nanomolar range partial agonist activity at the hMC1R is reported.

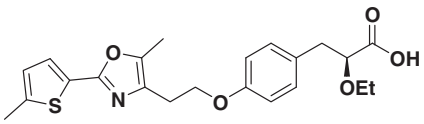

18d

Design and synthesis of a novel thiophene substituted oxazole derivatives are reported and their PPARα/γ agonistic activity has been evaluated. Lead compound **18d** has demonstrated potent antidiabetic and lipid lowering activity devoid of treatment related adverse effects and eventually emerged as very potent PPARα/γ dual agonist.

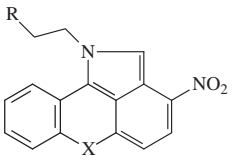

X= S, SO_2
R= $N(CH_3)_2$, $N(CH_2CH_3)_2$, $N(CH_2)_4$, $N(CH_2)_5$

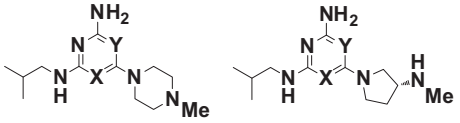

X = CH, Y = N
X = N, Y = CH
X = Y = CH

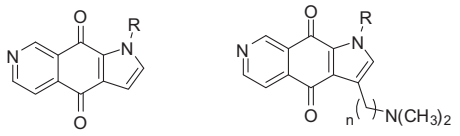

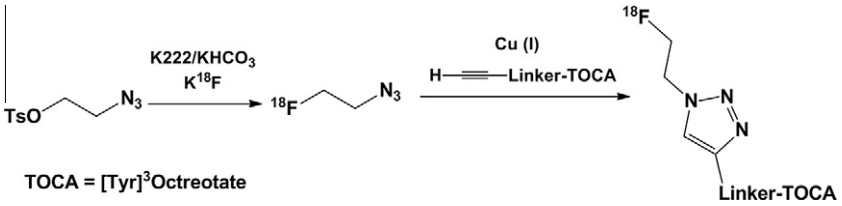

TOCA = [Tyr]^{3}Octreotate

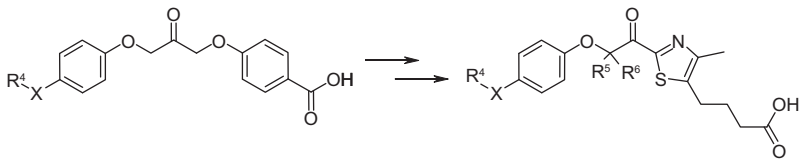

We report the design of novel, potent cPLA$_2\alpha$ inhibitors that possess an α-methyl-2-ketothiazole that acts as a serine-reactive moiety. We describe the optimization of the series for potency and metabolic stability towards ketone reduction. This was achieved by attenuating the reactivity of the ketone using a combination of electronic and steric effects.

The design of a new series of agonists of the orphan G-protein coupled receptor GPR119, starting from AR231453 is outlined. This resulted in the discovery of **3k** (APD668, JNJ-28630368), the first compound with this mechanism of action to be progressed into clinical development for the treatment of diabetes.

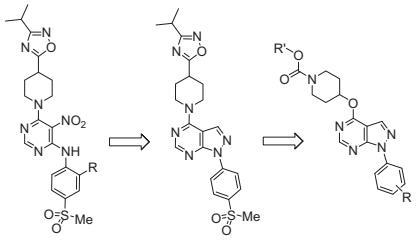

Described herein is the initial optimization of the screening hit (+/−) *N*-benzyl-4-heteroaryl-1-(phenylsulfonyl)-piperazine-2-carboxamide (**1**) that led to the discovery of the potent NS5B inhibitor (*S*)-*N*-*sec*-butyl-6-((*R*)-3-(4-(trifluoromethoxy)benzylcarbamoyl)-4-(4-(trifluoromethoxy)-phenylsulfonyl)-piperazin-1-yl)pyridazine-3-carboxamide (**2**).

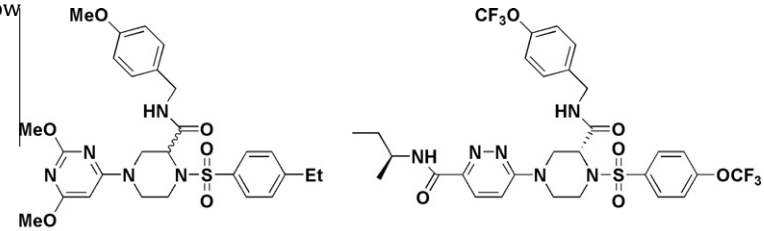

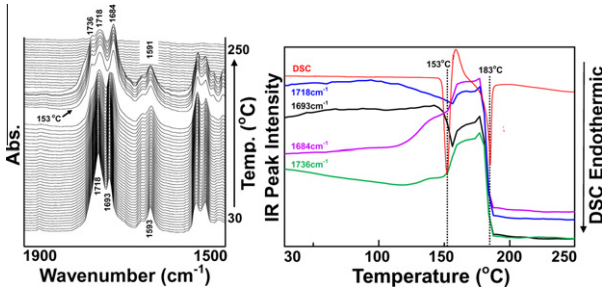

Thermal-dependent three-dimensional FTIR spectral plot of the physical mixture of IMC/SAC and its temperature-dependent changes in peak intensity of the specified IR bands.

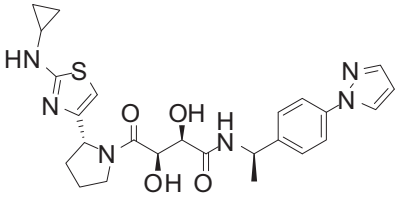

28

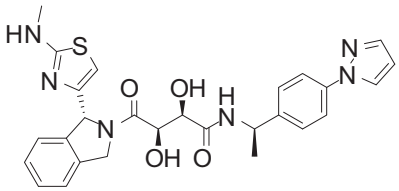

45

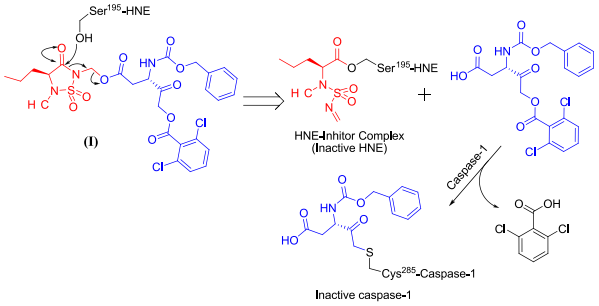

*Corresponding author
ⓘ+ Supplementary data available via ScienceDirect

COVER

Botulinum neurotoxins are the most deadly toxins known to man, approximately 10 million times more deadly than cyanide. Botulinum neurotoxins are classified by the US Centers for Disease Control (CDC) as bioterrorism agents. The etiological agent responsible for botulinum intoxication is a metalloprotease; as such this is a key therapeutic target. Currently, there are no approved pharmacological treatments for botulinum intoxication. Discovering molecules that could be used as a path forward for therapeutic development as botulinum protease inhibitors is tantamount. A benzylidene cyclopentenedione-based inhibitor was found to be the first affinity reagent to covalently modify the active site of botulinum neurotoxin A light chain metalloprotease. Its kinetic parameters are reported and such an approach for inhibition of this deadly neurotoxin. [Capková, K.; Hixon, M. S.; Pellett, S.; Barbieri, J. T.; Johnson, E. A.; Janda, K. D. *Bioorg. Med. Chem. Lett.* **2010**, *20*, 206.]

Indexed/Abstracted in: Beilstein, Biochemistry & Biophysics Citation Index, CANCERLIT, Chemical Abstracts, Chemistry Citation Index, Current Awareness in Biological Sciences/BIOBASE, Current Contents: Life Sciences, EMBASE/Excerpta Medica, MEDLINE, PASCAL, Research Alert, Science Citation Index, SciSearch, TOXFILE. Also covered in the abstract and citation database SCOPUS®. Full text available on ScienceDirect®

ELSEVIER

ISSN 0960-894X